Available online at www.sciencedirect.com
SCIENCE DIRECT
Polymer 47 (2006) 5402–5410
polymer
www.elsevier.com/locate/polymer

Enhanced fibrillation of LCP by $CaCO_3$ whisker in polysulfone matrix through increasing elongational stress

Jun Chen [a,b], Peng Chen [a,b], Lichuan Wu [a,b], Jun Zhang [a], Jiasong He [a,*]

[a] *Beijing National Laboratory for Molecular Sciences (BNLMS), Key Laboratory of Engineering Plastics, Joint Laboratory of Polymer Science and Materials, Institute of Chemistry, Chinese Academy of Sciences, Zhongguancun, Beijing 100080, China*
[b] *Graduate School, Chinese Academy of Sciences, Beijing 100039, China*

Received 2 March 2006; received in revised form 10 May 2006; accepted 21 May 2006
Available online 12 June 2006

Abstract

Induced by different fillers, various hydrodynamic effects enhance the fibrillation of liquid crystalline polymer (LCP) in in situ hybrid composites. Through choosing $CaCO_3$ whisker as the filler and polysulfone (PSF) as the matrix, the effect of the filler size and the affinity between components on the morphological evolution of LCP droplets has been investigated. In contrast to the spherical or ellipsoidal droplets of LCP formed in binary PSF/LCP blends, the fibrillation of LCP was promoted by the introduction of whisker particles in all ternary blends at shear rates studied. The analysis of the flow field indicated that the predominant factors promoting the fibrillation of LCP were the vortex enhanced and elongational stress increased by the whisker in the converging flow area at the entrance of capillary, rather than the viscosity ratio and capillary number.

Keywords: Polysulfone; Liquid-crystalline polymers (LCP); Whisker

1. Introduction

In recent years, great efforts have been made to investigate in situ hybrid composites, which combine the advantages of the reinforcing effect of inorganic fillers and the unique rheological properties of liquid crystalline polymer (LCP) [1–4]. The original motivation of introducing fillers into a thermoplastic polymer (TP)/LCP blend was to reduce the anisotropy and to improve further the mechanical properties of resultant composites [5]. However, in the further investigation, it is found that the morphological evolution of LCP domains becomes beyond the scope of the understanding of conventional binary TP/LCP blends. This is due to the additional hydrodynamic effects arising from the presence of fillers in in situ hybrid composites. To systemically illustrate these effects, many efforts have been made.

First, the different type and different size of fillers affect the morphological evolution of LCP in various ways. Nano-clay serving as a 'compatibilizer' in polyamide 6 (PA6)/LCP blends [6] promoted the fibrillation of LCP, and nano-SiO_2 through inhibiting the transesterification of LCP and polycarbonate (PC) enhanced the fibrillation of LCP [7].

Other than the nanometer-scale fillers, micrometer-scale or larger fillers seldom act as interfacial modifiers, but rather change the flow field and affect the LCP fibrillation in in situ hybrid composites. On the one hand, the addition of certain content of fillers changes the flow field in quantity. Chen et al. found that the addition of glass bead enhanced the LCP fibrillation in polycarbonate, due to an increased local shear prevailing between the neighboring beads [8,9]. On the other hand, the elongational flow developed through the micro-capillary formed by the stacked glass fibers and facilitated the LCP fibrillation in PC and PA6 by adding glass fiber (GF) [10,11]. Similar extensional flow was formed by the micro-rollers of the rotating glass bead (GB) in PC [9,12] and PA6 [13]. Obviously, the flow field was changed from shear flow to elongational flow in quality by fillers. So, in in situ hybrid composites containing LCP droplets and filler particles, extra hydrodynamic effects arise from the presence of filler particle and act on the morphological evolution of the LCP droplets.

However, different hydrodynamic effects arose from different fillers, due to their different shape and size. The rod-like filler (e.g. GF) developed elongational flow at

* Corresponding author. Tel.: +86 10 6261 3251; fax: +86 10 8261 2857.
E-mail address: hejs@iccas.ac.cn (J. He).

0032-3861/$ - see front matter © 2006 Elsevier Ltd. All rights reserved.
doi:10.1016/j.polymer.2006.05.044

the entrance of the instantaneously formed capillaries. The spherical filler such as GB produced local shear field from the rotation of glass beads. In addition, such a local shear was strengthened by the decrease of the gap between GB spheres at some extend, which was obtained through increasing the volume fraction of GB or decreasing its diameter or the both [9]. A comparable size of the average gap between GB with the diameter of the LCP droplet was the prerequisite for the generation of the local shear or elongational field. When the average gap of GB was decreased by highly packing of smaller GB, the shear flow actually changed, in quality, into an elongatioal flow. Too small gaps between smaller GB spheres made the spheres jam-packed and difficult to rotate individually. So, except the shape, the size of filler together with its content is also an important factor to induce additional hydrodynamic effects.

From above description, it is clear that the additional hydrodynamic effect arising from the presence of fillers is a process, which is affected by several factors. After investigating the effect of the diameter of spherical fillers on the LCP fibrillation, a new question is facing us: whether extra hydrodynamic effects may be induced by using smaller diameter of rod-like filler?

The whisker, the other rod-like filler, has been chosen to deepen the investigation of hydrodynamic driving forces enhancing the fibrillation in in situ hybrid composites. The whisker has the same shape as GF has, however, its diameter is about 1.0–2.0 μm, much smaller than GF, and its aspect ratio is lower than GF. If several whiskers stack on one another to form a micro-capillary, the diameter of this micro-capillary is about 0.5 μm, much smaller than the size of LCP droplets. It is impossible for the LCP droplets to pass through micro-capillaries formed by the stacked whiskers. Therefore, questions such as does the addition of this smaller rod-like filler affect the fibrillation of deformable LCP phase need their answers.

Secondly, the selective distribution of the filler in the polymer phases also influences the morphological evolution of LCP in in situ hybrid composites. Ding [13] found GB had strong affinity with LCP and migrated to the vicinity of LCP melt droplets, which resulted in the dispersion of LCP coils in the extensional flow field of 'roller machine' during the melt flow. Recently, it was observed that the morphological evolution of LCP domains in PC/LCP was affected by the addition of nano-SiO_2 [7]. The nano-SiO_2 selectively distributed at the PC/LCP interface, which inhibited the transesterification between PC and LCP and enhanced the fibrillation of LCP. However, in in situ hybrid composites, few reports were related to the selective distribution of fillers in the matrix, instead of at the interface or in the dispersed phase. By calculating interfacial tensions among components, it is found that polysulfone as the matrix can achieve the results that the whisker would selectively distribute within the PSF phase. What affects the fibrillation of LCP when the filler has a strong affinity with the matrix is another question for its answer.

In addition, whiskers are nearly free from internal defects such as dislocations owing to their small diameter; hence their strengths are close to the maximum theoretical value expected from the theory of elasticity [14]. Therefore, whiskers are used extensively as reinforcement materials for polymer matrix composites [15–16]. Furthermore, whiskers-reinforced polymer composites are especially suitable for preparing small but high-performance and high-dimension precision parts, which are generally difficult to reinforce by using fibers or fillers of large size. Therefore, choosing the whisker as a filler to study the hydrodynamic driving forces enhancing the LCP fibrillation has not only scientific significance but potential value for the industries.

To answer the above mentioned questions, the morphological evolution of LCP in in situ hybrid composites has been investigated by purposely choosing the filler and matrix polymer. The main aim is to reveal the hydrodynamic driving forces enhancing the LCP fibrillation in in situ hybrid composites containing deformable LCP phase and inorganic whisker fillers.

2. Experimental

2.1. Materials

Polysulfone (PSF) with an intrinsic viscosity of 0.54, produced by Shanghai Shuguang Chemical Factory, China, was used as the matrix. The LCP used was a commercial thermotropic liquid crystalline copolyester (Vectra A950, Hoechst Celanese, USA), comprising of 73 mol% hydroxybenzoic acid and 27 mol% hydroxynaphthoic acid, hereafter referred to as LCP. Its density in the solid state was 1.4 g/cm^3. $CaCO_3$ whiskers, kindly supplied by Qihai Haixing Science and Technology Development Ltd China., were used as the filler. More detailed physical properties of the $CaCO_3$ whiskers are listed in Table 1.

2.2. Blending

Prior to melt blending, all the materials were dried at 120 °C under vacuum for at least 24 h. All the composites were prepared by using a Haake rheomix 600 equipped with rotors. The blending temperature was 305 °C and the rotated speed was 50 rpm. The total blending time was 15 min. For decreasing the breakage of whiskers, PSF and LCP were melt blended first, followed by adding whiskers 5 min later. Two fixed PSF/LCP ratio 90/10 and 80/20 was adopted for all the blends, and the whisker content was taken as 0, 2.1, 4.1, 7.8, and 11.4 vol%, and 1.9, 4.2, 7.9, and 11.5 vol%, respectively.

Table 1
Physical properties of $CaCO_3$ whisker

Density (g/cm^3)	Diameter (μm)	Length (μm)	Specific surface area (m^2/g)	pH-value
2.86	1.0–2.0	10–30	Hydrophobic	7.0

2.3. Rheological measurement

The rheological property of all the pure components and composites was measured at 290 °C using a Rosand twin-bore advanced capillary rheometer, model RH7 (Bohlin Instruments Ltd, UK). The rheometer was equipped with two 1-mm capillary dies (a zero-length die and a 16 mm-length die) to carry out the Bagley correction for the end effects and the measurement of the elongational stress. The die entry angle was 180°. The extrudates at studied plunger speeds (i.e. different shear rates) were collected without any post-drawing for morphological analysis.

2.4. Morphological observation

The collected extrudates were immersed in *N*,*N*-dimethylacetamide (DMAc) for at least 24 h to dissolve the PSF matrix as the first step, followed by repeated washing the residue, and then were treated by using hydrochloric acid to dissolve the whisker for a clear show of the LCP particles. The residue LCP was coated with a thin layer of gold and observed on a scanning electron microscope (SEM Hitachi S-4300). Software, Photoshop 6.0 was used to measure the long axis a and the short axis b of LCP rod and fibrils. Consequently the aspect ratio (λ) was given by $\lambda = a/b$. For the case of $1 < \lambda \leq 5$, the volume of the ellipsoid V_e was calculated using Eq. (1); whereas for the case of $\lambda > 5$, the slender LCP particle was treated as a cylinder and its volume V_f was calculated using Eq. (2). By assuming that the LCP ellipsoid was deformed from spherical LCP droplet in molten state and the conservation of volume dominated the process, the number-average diameter (d_n) and volume-average diameter (d_v) of the initial LCP droplets can be calculated from V_e and V_f, respectively, using Eqs. (3)–(5). The d_n and d_v for each sample were obtained from at least 100 LCP particles.

$$V_e = \frac{\pi a b^2}{6} \tag{1}$$

$$V_f = \frac{\pi a b^2}{4} \tag{2}$$

$$d_i = 2 \times \left(\frac{3V_e}{4\pi}\right)^{1/3} \quad \text{or} \quad 2 \times \left(\frac{3V_f}{4\pi}\right)^{1/3} \tag{3}$$

$$d_n = \frac{\sum_i n_i d_i}{\sum_i n_i} \tag{4}$$

$$d_v = \frac{\sum_i n_i d_i^4}{\sum_i n_i d_i^3} \tag{5}$$

with n_i as the number of particles having diameter d_i.

2.5. Statistics on aspect ratio of whiskers

To calculate the distribution of aspect ratio of whiskers, the specimens were burnt at 650 °C for at least 6 h. The residue was dispersed in acetone, and collected and dried for SEM observation. From SEM micrographs, the size of whiskers was measured and their aspect ratio calculated.

3. Results and discussion

3.1. Aspect ratio evolution of whiskers through processing

A preliminary study was conducted to determine the breakage of whiskers after the processing. Fig. 1 shows the aspect ratio distribution of whiskers before and after the processing. The latter came from PSF composites containing LCP and whiskers. Through the blending, the average aspect ratio of whiskers decreased about 18% (from 11.8 to 9.6). However, those whiskers remained in the rod-like shape, and their aspect ratio satisfied the requirement of the present study. This is important for the later discussion.

3.2. Morphology evolution of dispersed LCP phase with increasing whisker content

Fig. 2 shows SEM images of LCP residues of PSF/LCP 90/10 blend and PSF/LCP/whisker composites containing 2.1, 4.1, 7.8, and 11.4 vol% whiskers, respectively. These samples were extruded from a capillary rheometer at the shear rate of $\sim 100\ s^{-1}$. For unfilled PSF/LCP blend, most LCP particles

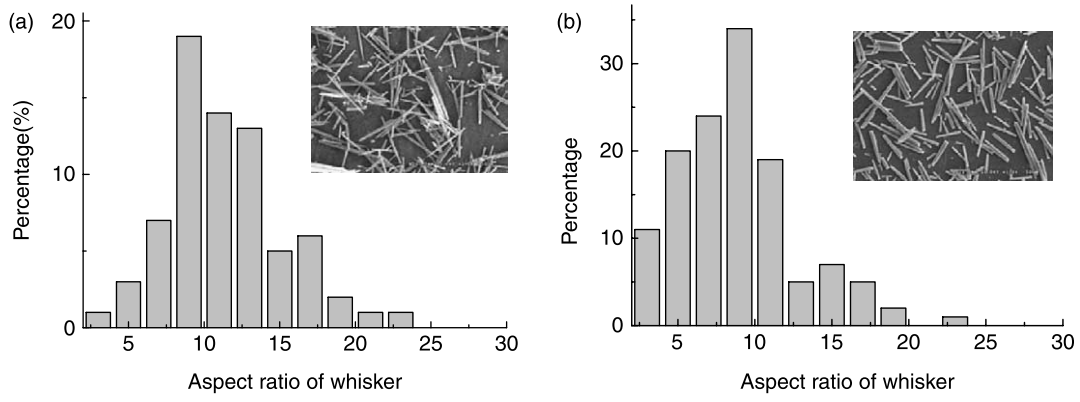

Fig. 1. Aspect ratio of whisker before (a) and after (b) blending, together with the SEM picture, and the weight ratio of PSF/LCP in the blends is 90/10 and whisker content is 11.4 vol%.

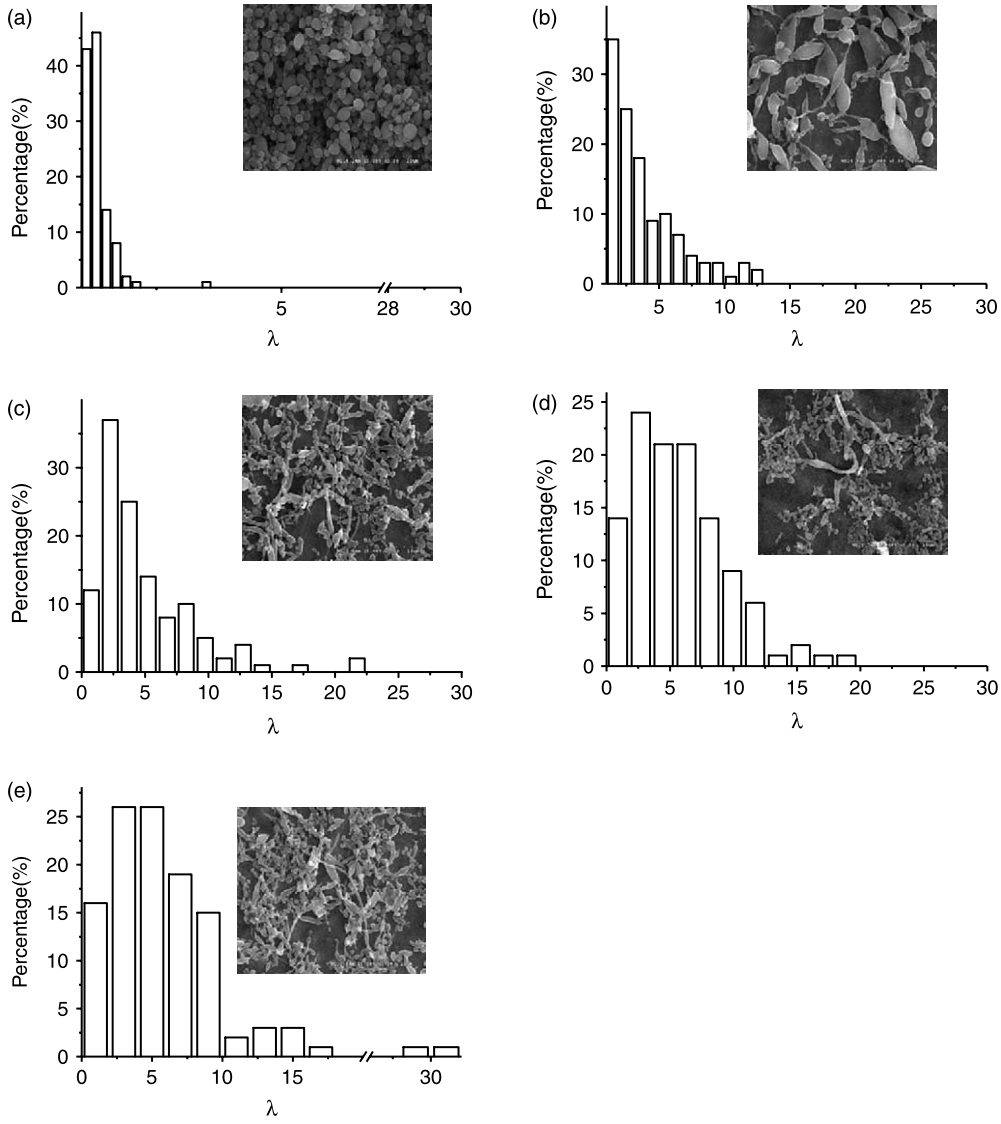

Fig. 2. SEM micrographs of residues extracted from the blends together with corresponding aspect ratio distribution of LCP particles, the weight ratio of PSF/LCP in the blends is always 90/10 and whisker content is: (a) 0 vol%, (b) 2.1 vol%, (c) 4.1 vol%, (d) 7.8 vol%, and (e) 11.4 vol%.

are spherical or ellipsoidal in shape (Fig. 2(a)), suggesting that the LCP droplets hardly deformed at such a low shear rate. Fig. 2 also gives corresponding aspect ratio distribution of LCP particles in all the samples. For binary PSF/LCP blend, the aspect ratio of 97% LCP particles is smaller than two. However, with whiskers added, even at the content of 2.1 vol%, there are some stretched LCP particles in the residue (Fig. 2(b)). For other filled PSF/LCP composites having whiskers up to 11.4 vol%, the amount of LCP rods and fibrils increases markedly. Obviously, the presence of whiskers in filled PSF/LCP composites promoted the deformation of dispersed LCP droplets into rods and fibrils of larger aspect ratios. This result indicates that in the capillary flow, whiskers promoted the deformation of LCP droplets.

To further illustrate this point, a series of samples loaded with different whisker contents and fixed PSF/LCP ratio at 80/20 was observed. The morphology of LCP particles extracted from these composites is shown in Fig. 3, together with the aspect ratio distribution of LCP particles. As shown in Fig. 3(a), both SEM picture and the statistic λ value of LCP indicate only $<8\%$ of LCP particles deformed into ellipsoids in the PSF/LCP blend. However, well-developed LCP fibrils were observed in whisker filled PSF/LCP blends. The higher the whisker concentration was, the better developed LCP fibrils were obtained. This further confirms that the presence of whisker promoted the fibrillation of LCP droplets in the PSF matrix by capillary flow.

On the basis of these SEM micrographs, the volume-average diameter (d_v) and the average aspect ratio (λ) of LCP particles were calculated to evaluate the morphological evolution caused by the introduction of whiskers. Fig. 4 shows plots of d_v and λ of the LCP particles vs. the volume fraction of whisker for composites of PSF/LCP 80/20 series extruded at the shear rate of 100 s^{-1}. This shows that, after adding a small amount of whiskers to the PSF/LCP blend, the average aspect ratio (λ) of LCP particles was significantly

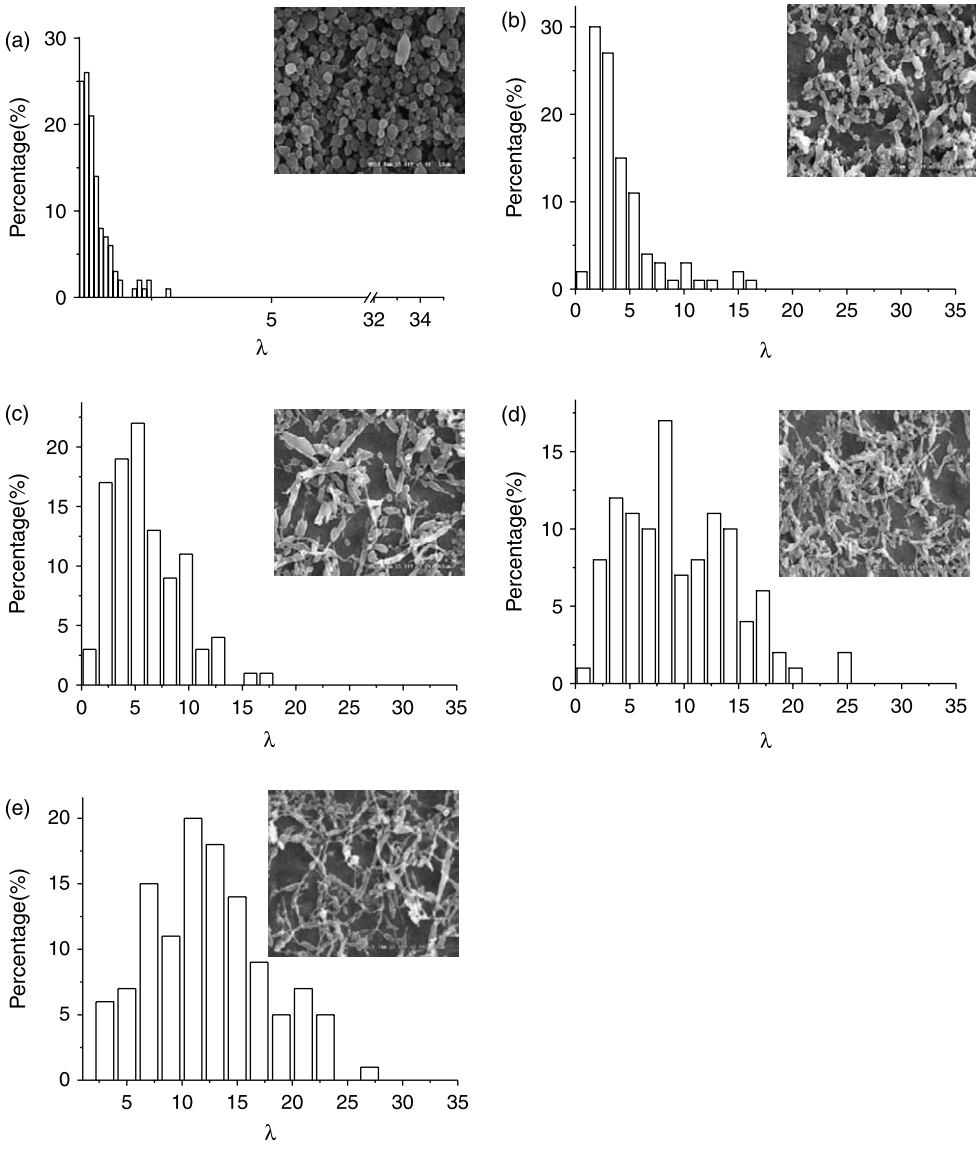

Fig. 3. SEM micrographs of residues extracted from the blends together with corresponding aspect ratio distribution of LCP particles, the weight ratio of PSF/LCP in the blends is always 80/20 and whisker content is: (a) 0 vol%, (b) 1.9 vol%, (c) 4.2 vol%, (d) 7.9 vol%, and (e) 11.5 vol%.

increased. Compared to the binary PSF/LCP blend, adding 2.1 vol% whisker increased the aspect ratio of LCP to three times, suggesting an enhanced fibrillation of LCP. With further addition of whiskers up to 11.5 vol%, a gradual increase in the aspect ratio is observed. At the maximum content 11.5 vol% of whiskers studied, the LCP average aspect ratio increases to 12.4, and the aspect ratio of about 91% LCP particles is larger than 5. At the same time, after adding a small amount of whiskers to the PSF/LCP blend, the volume-average diameter of LCP particles (d_v) is increased. With 1.9 vol% whisker added, d_v is about 1.2 times of the PSF/LCP blend. With further addition of whiskers up to 7.9 vol%, d_v of LCP appear a slight increase, and followed by a pronounced increase of d_v till 11.5 vol% whisker added. The increase of d_v together with the increase of aspect ratio of LCP particles suggests the increase of coalescence of LCP melt droplets by adding whiskers [8].

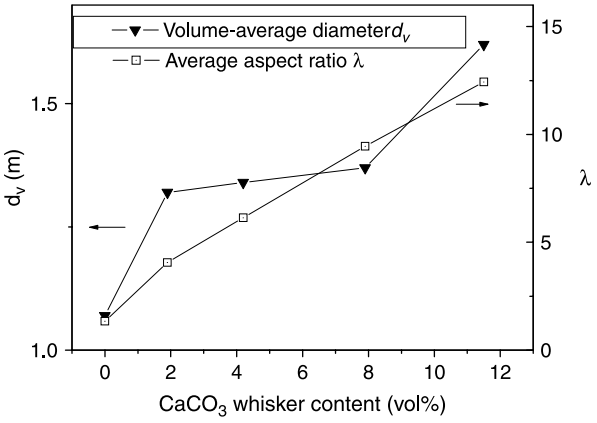

Fig. 4. Plot of volume average diameter and the average aspect ratio of LCP particle vs. the volume fraction of whisker at the shear rate of 100 s^{-1}, the weight ratio of PSF/LCP in the blends is 80/20.

All these results reveal that in the capillary flow, the deformation and fibrillation of LCP droplets were significantly promoted by adding whiskers into PSF/LCP blends, and more the whisker was added, the longer fibrils were obtained.

3.3. Mechanism of enhanced TLCP fibrillation

As described above, the introduction of whisker promoted the fibrillation of LCP in the PSF/LCP/whisker composite. How did the whisker affect the morphological evolution of LCP was a critical issue to reveal the hydrodynamic effect.

3.3.1. Influence of viscosity ratio on LCP fibrillation

It is commonly known that the deformation of LCP droplets is governed by several factors. Among these factors, the viscosity ratio of components was one of the important rheological parameters determining the morphology in immiscible blends containing LCP [17,18]. Several authors [19–22] have reported that the fibrous microstructure of LCP was obtained only at the viscosity ratio of the dispersed LCP phase to the matrix below unity. For a bi-phase blend consisting of a continuous phase and a dispersed one, the viscosity ratio of melts is defined as:

$$P = \frac{\eta_d}{\eta_m} \tag{6}$$

Here, η is the viscosity, and the subscripts d and m refer to the dispersed phase and the matrix, respectively. For composites consisting of three components, however, different ways were used to calculate the viscosity ratio. Lee et al. [23] adopted the viscosity of PP/SiO_2 composites as η_m for PP/SiO_2/LCP ternary systems. In another way, Jansen et al. [24] introduced a rescaled viscosity ratio with replacing the continuous phase viscosity η_m by the average emulsion viscosity η_{em} to account for the breakup of droplets in concentrated emulsions. In the present study, we started with the affinity among PSF, LCP and the whisker to discuss the distribution of the dispersed LCP phase and determine η_m later.

Premphet and Horanont [25] found that in filled blends with two immiscible polymers their filler distributed selectively in the polymer-phase, with which it had the lowest interfacial tension. An extension of this qualitative approach has been provided by Sumita et al. [26]. They introduced a wetting coefficient, Wa, which allows predicting the selectivity of filler.

$$\mathrm{Wa} = \frac{\gamma_{\text{filler–B}} - \gamma_{\text{filler–A}}}{\gamma_{\text{A–B}}} \tag{7}$$

Table 2
Surface tension of polymers and $CaCO_3$ whisker [34–36]

	Surface tension (mN/m)		
	Total (γ)	Disperse component (γ^d)	Polar component (γ^p)
PSF	37.7	26.0	11.7
LCP	31.25	24.49	6.76
$CaCO_3$ whisker	207.9	54.5	153.4

where, $\gamma_{\text{filler-A}}$ and $\gamma_{\text{filler-B}}$ are the interfacial tension between the fillers and polymer A or B, and $\gamma_{A–B}$ is the interfacial tension between polymer A and B. If $\mathrm{Wa} > 1$, the filler distributes within A-phase; if $-1 < \mathrm{Wa} < 1$, the filler is located at the interface; if $\mathrm{Wa} < -1$, the filler is selective for the B-phase. If we know the values of the interfacial tension such as $\gamma_{\text{PSF-LCP}}$, $\gamma_{\text{PSF-Whisker}}$ and $\gamma_{\text{LCP-Whisker}}$, we can calculate the value of Wa. In this paper, A is PSF and B is LCP.

The interfacial tensions between the components are determined with harmonic mean equation and geometric mean equation, respectively [27].

$$\gamma_{\text{PSF–LCP}} = \gamma_{\text{PSF}} + \gamma_{\text{LCP}} - \frac{4\gamma^d_{\text{PSF}}\gamma^d_{\text{LCP}}}{\gamma^d_{\text{PSF}} + \gamma^d_{\text{LCP}}} - \frac{4\gamma^p_{\text{PSF}}\gamma^p_{\text{LCP}}}{\gamma^p_{\text{PSF}} + \gamma^p_{\text{LCP}}} \tag{8}$$

$$\gamma_{A–B} = \gamma_A + \gamma_B - 2\left(\gamma^d_A\gamma^d_B\right)^{1/2} - 2\left(\gamma^p_A\gamma^p_A\right)^{1/2} \tag{9}$$

where γ_{PSF} and γ_{LCP} are the surface tensions of PSF and LCP, the superscripts d and p denote the dispersion and polar components of the surface tension, the subscripts A and B denote polymers and filler, respectively. Corresponding values of the surface tension are taken from the literature [28–30] and listed in Table 2.

According to Eqs. (8) and (9), the values of interfacial tensions $\gamma_{\text{PSF–LCP}}$, $\gamma_{\text{PSF–whisker}}$, and $\gamma_{\text{LCP–whisker}}$, are given in Table 3. It shows that the interfacial tension between the whisker and LCP, $\gamma_{\text{LCP–whisker}}$ is by 16.2 larger than the corresponding value between the whisker and PSF, $\gamma_{\text{PSF–whisker}}$. According to the Refs. [25,31], this indicates an affinity of the whisker to the PSF larger than to LCP melt in the composite. The concept of the wetting coefficient also confirms this tendency: Eq. (7) yields a wetting coefficient of 11.8. Therefore, the whisker would distribute selectively in the PSF phase and the PSF/whisker composite could be regarded as the matrix (i.e. an equivalent medium) for the calculation of the viscosity ratio in our studied system.

SEM observation confirmed the selective distribution of whiskers in PSF matrix. The morphology of frozen PSF/LCP/whisker composites after extrusion in the capillary experiments is shown in Fig. 5. There are two dispersed phases. The larger one as regular hexagons pointed by the arrow is $CaCO_3$ whisker, which has been identified by energy dispersive X-ray (EDX) element analysis (the EDX element maps are not shown here). In this picture, we can clearly find that the whisker selectively located in the PSF phase, and the interfacial adhesion between the whisker and LCP was very well. This phenomenon was consistent with the above calculation showing a good affinity of the $CaCO_3$ whisker with PSF.

Table 3
Interfacial tension between the possible polymer–polymer and polymer–filler pairs

Possible pairs	Interfacial tensions (mN/m)
PSF–LCP	1.37
PSF–whisker	85.6
LCP–whisker	101.8

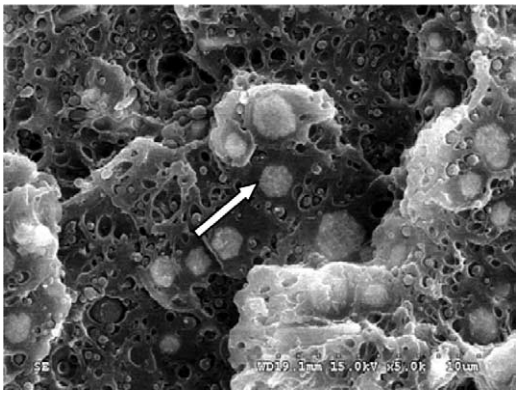

Fig. 5. SEM pictures of cryo-fractured surfaces of the PSF/LCP/whisker extrudates, the weight ratio of PSF/LCP in the blends is 90/10 and whisker content is 11.4 vol%.

However, the relatively smaller dispersed particles were the LCP phase, which has coarse interface with PSF. Therefore, in the present study, the PSF/whisker acts as an equivalent medium on the morphology evolution of the LCP phase.

Fig. 6 shows the viscosity of PSF/whisker composites as a function of whisker content at 290 °C and shear rate of $\sim 100\ s^{-1}$. It is shown that the viscosity of PSF/whisker composites increases clearly with increasing the whisker content. According to this analysis, the whisker acted as a viscosity thickening agent, which favored the fibrillation of LCP droplets. However, the calculation of the viscosity ratio of the LCP to the matrix showed that the change of viscosity ratio was relatively little (Table 4). As Table 4 shows, with increasing whisker content, the viscosity ratio decreased mostly about one half. However, with the increase of whisker content from 0 to 11.5%, the average aspect ratio of LCP increased about 9 times (Fig. 4). Yet, we doubted whether the viscosity ratio remained the only factor to control the LCP morphology with the presence of whisker.

3.3.2. The effects of capillary number on the fibrillation of LCP

To illustrate this problem, the capillary number, Ca, which is defined as the ratio of the shear stress acting on the LCP droplet by an external flow field to the interfacial tension, which resists the deformation of the spherical droplet, has been calculated [32]

$$\mathrm{Ca} = \frac{\eta_b \dot{\gamma} d\left[1-(4\phi_d\phi_m)^{0.8}\right]}{2\sigma}\,\frac{16p+16}{19p+16} \tag{10}$$

where η_b is the blend viscosity, $\dot{\gamma}$ is the shear rate, d is the diameter of the dispersed phase droplet, σ is the interfacial tension, p is the viscosity ratio, ϕ_d the volume fraction of the dispersed phase, and ϕ_m the volume fraction of the matrix.

According to the Eq. (10) the values of capillary number of the present system have been calculated and listed in Table 4. It shows that the capillary number of PSF/LCP/whisker composites increases with increasing whisker content. This means that the deformation of LCP droplets would have become easier with the introduction of whiskers. However, the increase in Ca with the whisker content is very small. As the whisker content increased from 0 to 1.9 and 4.2 vol%, the capillary number changed from 33.8 to 36.5 and 37.4, respectively. This little difference less than 10% could not increase the average aspect ratio of LCP about three to fivefold. Therefore, the viscosity ratio of LCP to the matrix was not the predominant factor determining the fibrillation of LCP in the present system. Induced by the presence of whisker, there must be other factors governing the fibrillation of LCP phase, which is beyond the scope of conventional understanding of binary PSF/LCP bend.

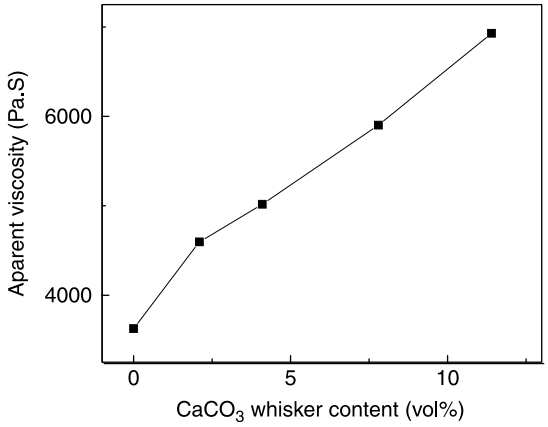

Fig. 6. Effect of whisker content on viscosity of PSF/whisker composite at a shear rate of 100 s^{-1} at 290 °C.

3.3.3. The increase of elongational field promoting the fibrillation of LCP

It should be noticed that the fibrillation of the droplets was a process affected by several factors, especially in the ternary systems. The filler introduced into in situ hybrid composites not only acts as a viscosity thickening agent, but also changes the flow field and affects the LCP fibrillation. In addition to this, the different shape of fillers may result in different hydrodynamic effects [8–13]. Therefore, it should be investigated how did the whisker, with its unique shape and aspect ratio, affect the flow field and act on the morphological evolution of LCP.

It is widely accepted that the elongational flow developed at the entry of the capillary is mainly responsible for the LCP fibrillation during a capillary extrusion [33]. Therefore, the stress field at the entrance of the capillary should be measured. Using the Cogswell [34] and Binding [35] analysis, the elongational properties of materials can be obtained from the pressure loss (ΔP_{ent}) in the converging flow region in the entrance zone of a capillary die. Obtaining the ΔP_{ent} is the key problem to provide the indication of the extensional character of the fluid. The most common method for determining ΔP_{ent} is through the Bagley end correction. It includes extrapolating the measured pressure drop across multiple capillaries of the same diameter and different *L*/*D* ratios of the zone. This extrapolated quantity then represents ΔP_{ent} for the given contraction ratio. Some factors, which may produce errors in the value of ΔP_{ent}, such as the viscous heating and wall slip can be significantly

Table 4
Effect of whisker content on the viscosity ratio of the LCP to the PSF/whisker composites and capillary number at a shear rate of 100 s^{-1} and the weight ratio of PSF/LCP in the blends is 80/20

Whisker content (vol %)	0	1.9	4.2	7.9	11.5
Viscosity ratio	0.052	0.041	0.037	0.031	0.027
Capillary number	33.8	36.5	37.4	40.5	54.2

lessened by using a very short die ($L/D \approx 0$). Therefore, using converging flow of the capillary for measuring elongational properties of fluid is a convenient approach broadly applied by many authors [36–40].

In the present study, the zero-length die and a 16 mm-length die were used to measure the elongational stress of entrance region of capillary. The plot of elongational stress vs. the volume fraction of whisker at ca. 100 s^{-1} is shown in Fig. 7. For comparison, the average aspect ratio of LCP particles is also shown. It is clear that the elongational stress of entrance region of capillary increases significantly with the whisker content. Compared to the PSF/LCP 80/20 blend, the hybrid composite containing 11.5 vol% whisker has a 347 kPa increase of elongational stress (Fig. 7(a)). Furthermore, the PSF/LCP 90/10 system have a similar trend, i.e. the addition of 11.4 vol% whisker increases elongational stress from 841 to 1166 kPa (Fig. 7(b)). Therefore, the extra hydrodynamic effect

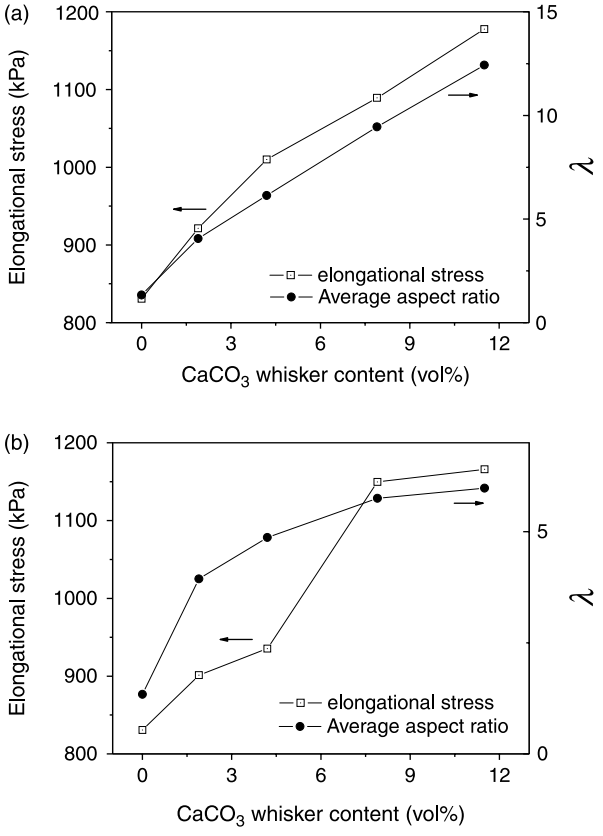

Fig. 7. Plot of elongaional stress at the entrance of capillary die and the average aspect ratio of LCP particle vs. the volume fraction of whisker at the shear rate of 100 s^{-1}, the weight ratio of PSF/LCP in the blends is: (a) 80/20 and (b) 90/10.

arises at the inlet region of the capillary die through the introduction of whiskers. This extra tensile stress, once generated, affected not only the properties of the polymer matrix, but also the morphology of the dispersed LCP phase. The average aspect ratio of LCP (Fig. 7) increases with the elongational stress in the converging flow region in the entrance zone of a capillary die. It is well known that the elongational stress is the most favorable factor to promote the fibrillation of LCP in in situ composites [10–13,33,41]. So with the introduction of whisker to the PSF/LCP blend, the extra elongational stress was the predominant factor to promote the LCP fibrillation and increase the average aspect ratio of LCP from 1.3 to 12.4.

Now, the discussion should move to a further question how was this extra elongational stress generated. To answer this question, let us have a look of thermoplastic/rod-like particle systems. Although many authors [42,43] have investigated fluid streamlines, based on the assumption that the stress field remains unaltered by the presence of fibers, more and more researchers clearly show from their predictions and experiments that the presence of fiber drastically changed the flow field. Thomasset [44] found that in concentrated situations fibers formed bundles, which could generate large energy dissipation and oscillations in the entry flow. Interesting simulation results for suspensions of large aspect ratio fibers in Newtonian fluids were obtained by Chiba et al. [45], and showed that the presence of long and rigid fibers induced drastic changes to the kinematics of an axisymmetric entry flow. These indicate the effect of the rod-like filler on the flow velocity and stress fields is very important, especially in the axisymmertric entry flow region.

A detailed study of the inlet regions was performed by Tang and Altan [46] and showed that the inlet length increased significantly when fibers were added to the flow. More importantly, for the numerical simulation of the flow of a fiber suspension through an axisymmetric tubular contraction, larger corner recirculating vortices were predicted by Lipscomb et al. [47] even for very low volume fraction. Chiba et al. [45] confirmed and extended these results, and clearly showed that the corner vortex grew as the volume fraction of fibers increased. In other words, the presence of fibers increases the corner vortex and correspondingly to increase the tensile stress at the inlet region.

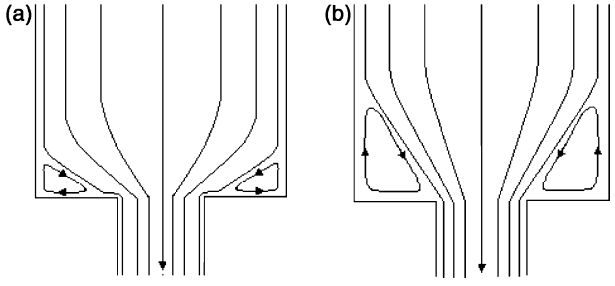

Fig. 8. Schematic diagram of the evolution of the flow filed in the converging flow region in the entrance zone of the capillary die: (a) unfilled (b) rod-like filler filled.

Fig. 8 schematically illustrates the appearance of additional tensile stress produced by vortex enhancement in the converging flow region in the entrance zone of a capillary die. Fig. 8(a) shows the flow field of an unfilled fluid and Fig. 8(b) of rod-like filler filled one. It is accepted that the entry flow can be modeled as a one-dimensional acceleration problem [48]. And it is this acceleration of the fluid through the contraction that results in the appearance of elongational field. Due to the presence of fibers, the vortex enhancement phenomenon would be occurred in the converging area at the capillary entrance, see Fig. 8(b). This vortex enhancement resulted in the enlargement of the acceleration zone and the increase of velocity of the fluid, which in turn increased the strength of the elongational field and the elongatioal stress in the entrance of capillary.

From above discussion, we understand how the addition of whiskers altered the flow field and accordingly influenced the morphology of LCP in in situ hybrid composites. That is in the converging area at the capillary entrance, extra hydrodynamic effects arose from the presence of rigid whiskers. This rigid rod-like filler altered the flow field and increased the tensile stress at the capillary entrance. Therefore, in our PSF/whisker/LCP composites, the addition of whiskers increased the efficiency of elongational field in the entry of capillary, and resulted in the fibrillation of LCP.

4. Conclusions

The fibrillation of LCP in the PSF matrix at different LCP/PSF ratios was examined, with the addition of various contents of whiskers. LCP mainly formed spheres and less-deformed ellipsoids in PSF/LCP binary blends at the shear rates studied. However, after the whisker was added into the binary blends, LCP fibrils with large aspect ratios were generated in all the hybrid composites; and the more whiskers were added, the larger aspect ratio of LCP was obtained. Although the decreased viscosity ratio by the whisker addition might favor the LCP fibrillation, the calculation of the capillary number showed that the change of viscosity ratio was not the predominant factor controlling the fibrillation of LCP in the present hybrid composite. The results measured from the capillary entrance showed that the introduction of whiskers increased the elongational stress in the entrance of capillary. The analysis of flow field confirmed that the presence of rigid whiskers altered the flow field and enhanced the vortex in the converging flow area at the entry of the capillary. It is this vortex enhancement that resulted in the increase of the elongational stress and promoted the fibrillation of the LCP droplet in PSF/LCP/whisker systems.

Acknowledgements

This work was supported by the National Nature Science Foundation of China, Grant no. 50233010.

References

[1] He J, Zhang H, Wang Y. Polymer 1997;38:4279–83.
[2] He JS, Wang YL, Zhang HZ. Compos Sci Technol 2000;60:1919–30.
[3] Tjong SC, Meng YZ. Polymer 1999;40:1109–17.
[4] Shumsky VF, Getmanchuk IP, Lipatov YS. J Appl Polym Sci 2000;76:993–9.
[5] Bafna SS, DeSouza JP, Sun T, Baird DG. Polym Eng Sci 1993;33:808–18.
[6] Zhang B, Ding Y, Chen P, Liu C, Zhang J, He J, et al. Polymer 2005;46:5385–95.
[7] Wu L, Chen P, Zhang J, He J. Polymer 2006;47:448–56.
[8] Chen P, Wu L, Ding Y, Zhang J, He J, Compos Sci Technol 2006;66:1564–74.
[9] Chen P, Chen J, Zhang B, Zhang J, He J. J Polym Sci, Part B: Polym Phys 2006;44:1020–30.
[10] Zheng X, Zhang B, Zhang J, Xue Y, He J. Int Polym Proc 2003;18:3–11.
[11] Zheng X, Zhang J, He J. J Polym Sci, Part B: Polym Phys 2004;42:1619–27.
[12] Chen P, Zhang J, He J. Polymer 2005;46:7652–7.
[13] Ding Y, Zhang J, Chen P, Zhang B, Yi Z, He J. Polymer 2004;45:8051–8.
[14] Courtney TH. Mechanical behavior of materials. New York: McGraw Hill; 1990 p. 83–84.
[15] Hao X, Gai G, Lu F, Zhao X, Zhang Y, Liu J, et al. Polymer 2005;46:3528–34.
[16] Sriupayo J, Supaphol P, Blackwell J, Rujiravanit R. Polymer 2005;46:5637–44.
[17] Saengsuwan S, Bualek-Limcharoen S, Mitchell GR, Olley RH. Polymer 2003;44:3407–15.
[18] Wang H, Tao X, Newton E, Chung TS. Polym J 2002;34:575–83.
[19] He J, Bu W, Zhang H. Polym Eng Sci 1995;35:1695–704.
[20] Sukhadia AM, Done D, Baird DG. Polym Eng Sci 1990;30:519–26.
[21] Berry D, Kenig S, Siegmann A. Polym Eng Sci 1991;31:451–8.
[22] Berry D, Kenig S, Siegmann A. Polym Eng Sci 1991;31:459–66.
[23] Lee MW, Hu X, Yue CY, Li L, Tam KC, Nakayama K. J Appl Polym Sci 2002;86:2070–8.
[24] Jansen KMB, Agterof WGM, Mellema J. J Rheol 2001;45:227–36.
[25] Premphet K, Horanont P. Polymer 2000;41:9283–90.
[26] Sumita M, Sakata K, Asai S, Miyasaka K, Nakagawa H. Polym Bull 1991;25:265–71.
[27] Wu S. Polymer interface and adhesion. New York: Marcel Dekker; 1982.
[28] Ma K, Chung TS, Good RJ. J Polym Sci, Part B: Polym Phy 1998;36:2327–37.
[29] Pukanszky B, Fekete E. Adv Polym Sci 1999;139:109–53.
[30] Zhang J, He J. Polymer 2002;43:1437–46.
[31] Schuster RH, Issel HM, Peterseim VI. Rubber Chem Technol 1996;69:769–80.
[32] Serpe G, Jarrin J, Dawans F. Polym Eng Sci 1990;30:553–65.
[33] He J, Bu W. Polymer 1994;35:5061–6.
[34] Cogswell FN. Polym Eng Sci 1972;12:64–73.
[35] Binding DM. J Non-Newtonian Fluid Mech 1988;27:173–89.
[36] Thomasset J, Carreau PJ, Sanschagrin B, Ausias G. J Non-Newtonian Fluid Mech 2005;125:25–34.
[37] Clarke J, Petera J. J Appl Polym Sci 1997;66:1139–50.
[38] Eggen S, Hinrichsen EL. Polym Eng Sci 1996;36:410–24.
[39] Gupta M. Adv Polym Technol 2002;21:98–107.
[40] Pickles AP, Gibson AG. Polym Eng Sci 1996;36:23–33.
[41] Kohli A, Chung N, Weiss RA. Polym Eng Sci 1989;29:573–80.
[42] Givler RC, Crochet MJ, Pipes RB. J Compos Mater 1983;17:330–41.
[43] Goddard JD, Huang YH. J Non-Newtonian Fluid Mech 1983;13:47–62.
[44] Thomasset J, Grmela M, Carreau PJ. J Non-Newtonian Fluid Mech 1997;73:195–203.
[45] Chiba K, Nakamura K, Boger DV. J Non-Newtonian Fluid Mech 1990;35:1–14.
[46] Tang L, Altan MC. J Non-Newtonian Fluid Mech 1995;56:183–216.
[47] Lipscomb GG, Denn MM, Hur DU, Boger DV. J Non-Newtonian Fluid Mech 1988;26:297–325.
[48] Bulters MJH, Meijer HEH. J Non-Newtonian Fluid Mech 1990;38:43–80.